Electronic Supplementary Material (ESI) for RSC Advances.

Supporting Information

Synthesis and characterization of geometrically tunable nano-size hollow silicate particles and their dip-coating prepared films for thermal management applications

Raymond V.Rivera Virtudazo[a], Ye Lin[b], and Rudder T. Wu*[c]

[a]*Global Research Center for Environment and Energy Based on Nanomaterials Science (GREEN), National Institute for Materials Science (NIMS), Namiki, Tsukuba, Ibaraki 305-0044 Japan*

[b]*School of Municipal and Environmental Engineering, Shenyang Jianzhu University, Shenyang China*

[c]*National Institute for Materials Science (NIMS), Tsukuba, Ibaraki 305-0044 Japan*

*corresponding author. TEL: +81-(0)29-860-4702 FAX: +81-(0)29-860-4984
*E-mail: WU.rudder@nims.go.jp

ABBREVIATIONS

RT, CC room temperature; DDA, CC drug delivery application; NHSP, CC nano sized hollow nanoparticles; EtOH, CC ethanol; SiO_2, CC silica, silicate; TEOS, CC tetraethyl orthosilicate; XRD, CC x-ray diffraction; NH_4OH(aq), ammonia solution; STEM, CC scanning/transmission electron microscopy; TEM, CC transmission electron microscopy; TG, CC thermogravimetric analysis; BJH, CC Barrett-Joyner-Halenda method; BET, CC Brunauer-Emmett-Tellers Method.

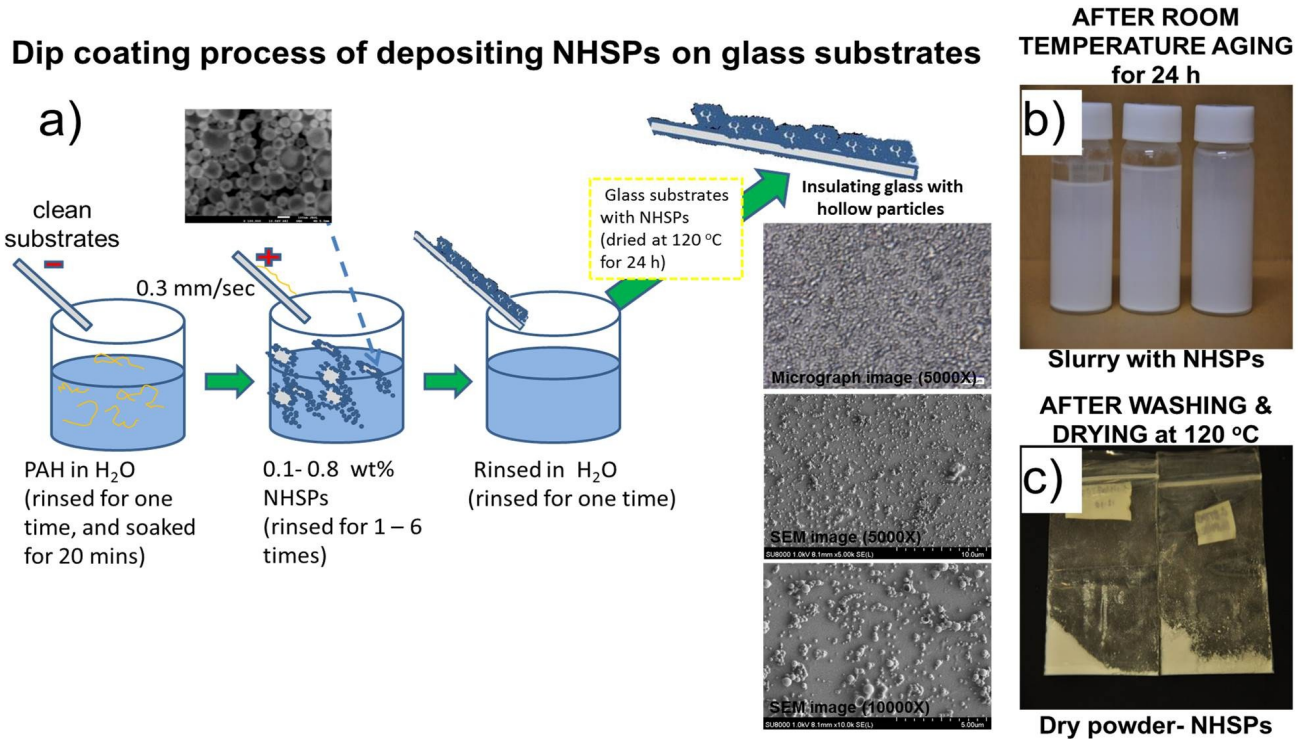

Fig. S 1 (a) Dip coating processeses of preparing NHSPs coated glass substrates . Images of NHSPs (b) suspended in slurry and (c) in dried form

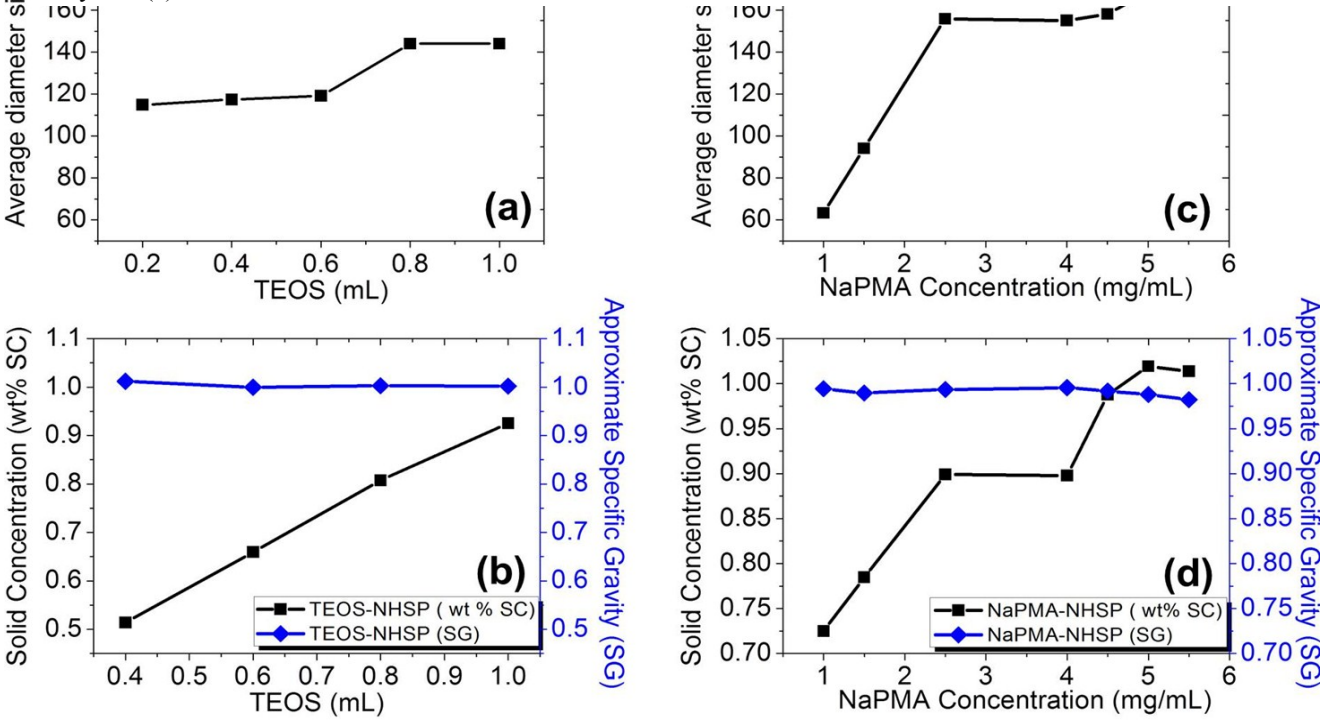

Fig. S 2 (a ,c) Average particles size distribution with (b,d) average solid concentrations (sc , ■) and approximate specific gravity (sg, ◆) of NHSPs powder samples upon varying (a,b) X-TEOS and (c, b) Y-NaPMA concentrations.

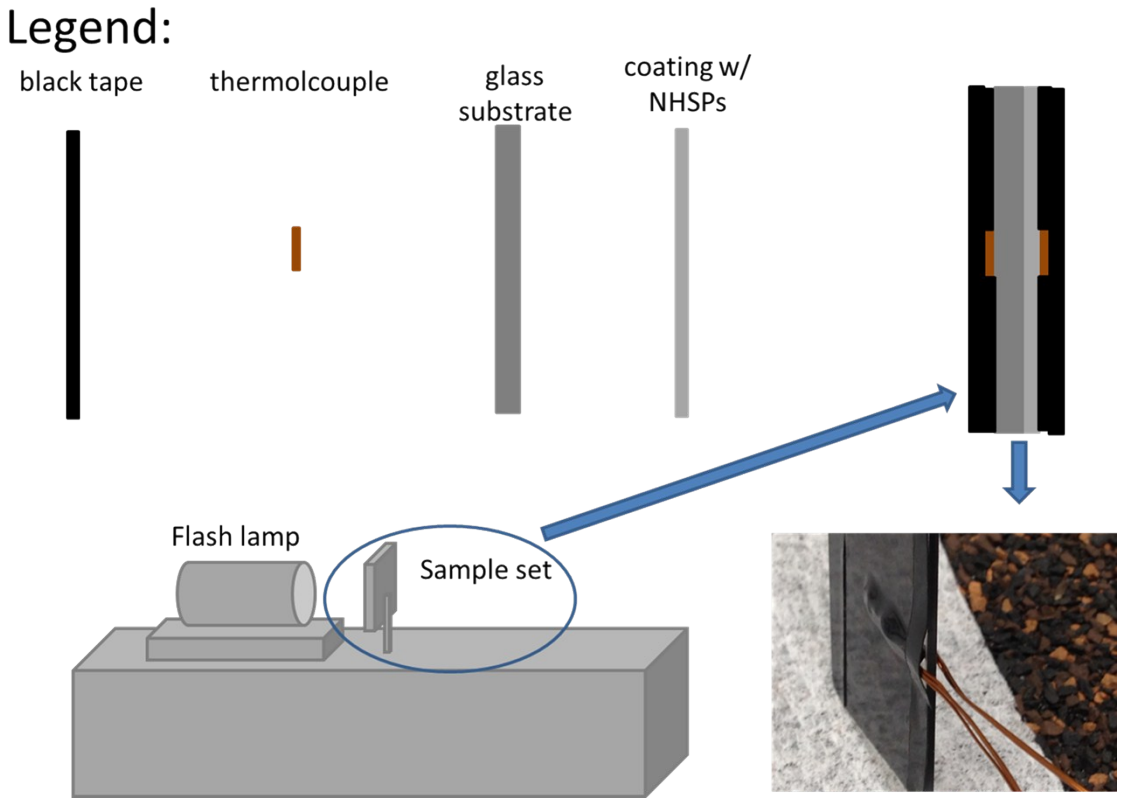

Fig. S 3 Test samples covered with water-resistant black tape for thermal characterization using a xenon flash lamp set-up.

Fig. S 4 Test samples covered with water-resistant black tape for thermal characterization

$$q = \frac{kA\Delta T}{\Delta x}$$

q and A : heat flux & Area of the heat flux received, respectively
ΔT : temp. difference,
Δx : thickness of the samples
k : thermal conductivity of the material / sample

Calculation for k (thermal conductivity)
Since,
q is constant
k_G is glass (1.05 W/mK)
k_{CG} is NHSPs coated glass
$A_G = A_{CG}$ is the area of the xenon flash light beam

From the equation $q = \frac{kA\Delta T}{\Delta x}$

where, $q_G = q_{CG}$

Then k_G is known
$\Delta x_G, \Delta x_{CG}$ are measured by an electronic caliper
ΔT is measured by thermocouples
So

$$k_{CG} = \frac{k_G \Delta T \Delta x_{CG}}{\Delta x_G}$$

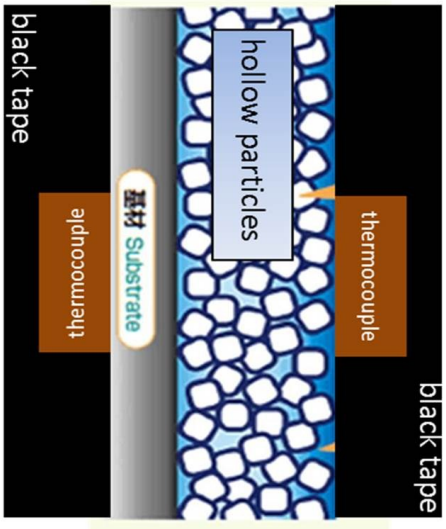

Real-time temperature monitored and recorded using tracking software, KIDS (CHINO Corp)

- Light source: xenon flash lamp with build in reflector (Hamamatsu Photonics)
- Spectral distribution: 190 nm - 2000 nm, maximum average input 1J/ flash and 60 W for continuous flashing
- Max. flashing frequency: 60 Hz
- Continuous flashing frequency with the maximum intensity used to heat up the samples
- thermocouples are placed on both sides of the samples

Fig. S 5 Sample calculation for thermal conductivity (k) of the material

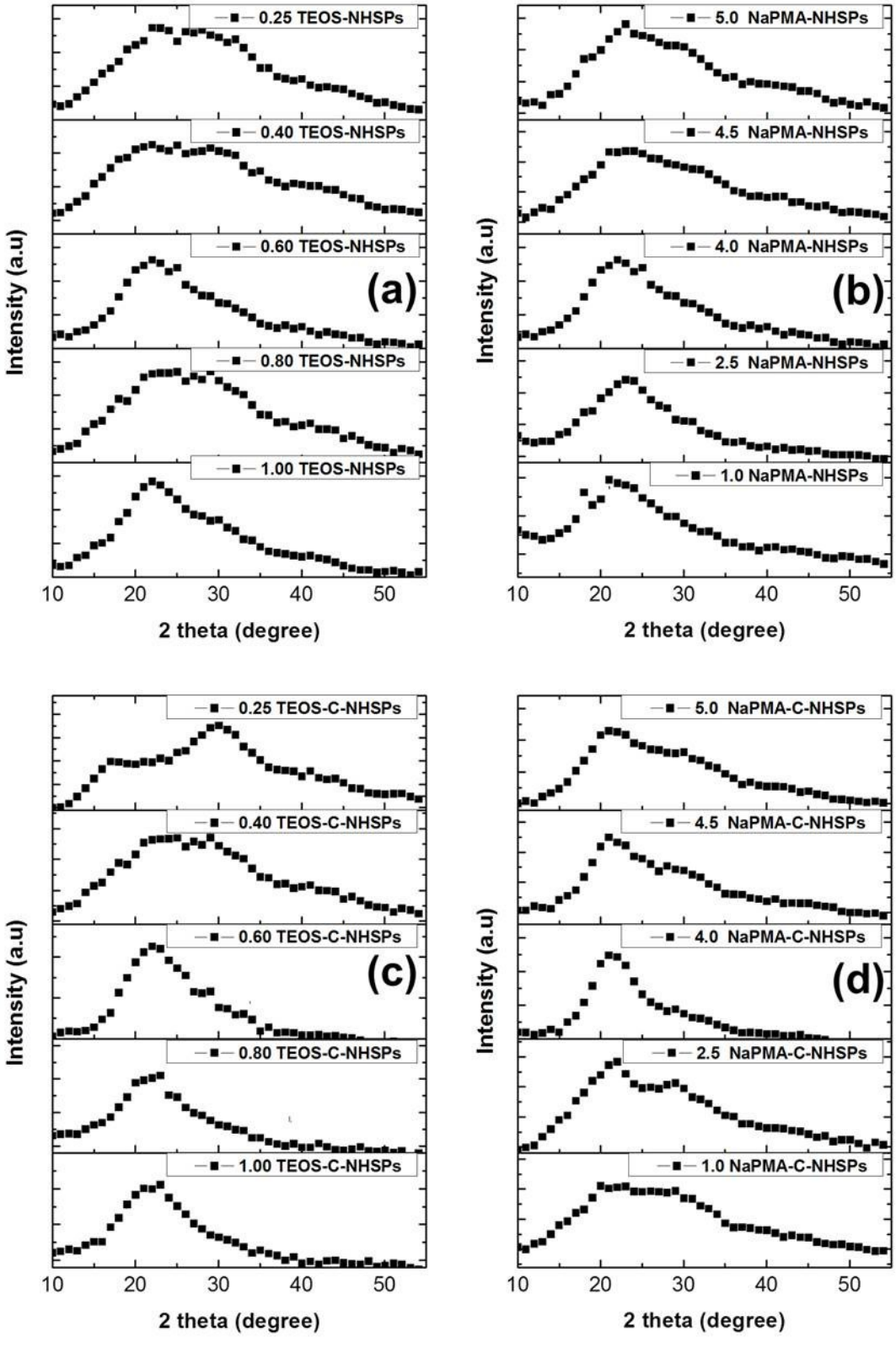

Fig. S 6 Amorphous XRD spectra of NHSPs with varying (a) X-TEOS and (b) Y-NaPMA concentrations. Also, amorphous XRD spectra of calcined-NHSPs with varying (c) X-TEOS-C and (d) Y-NaPMA-C concentrations.

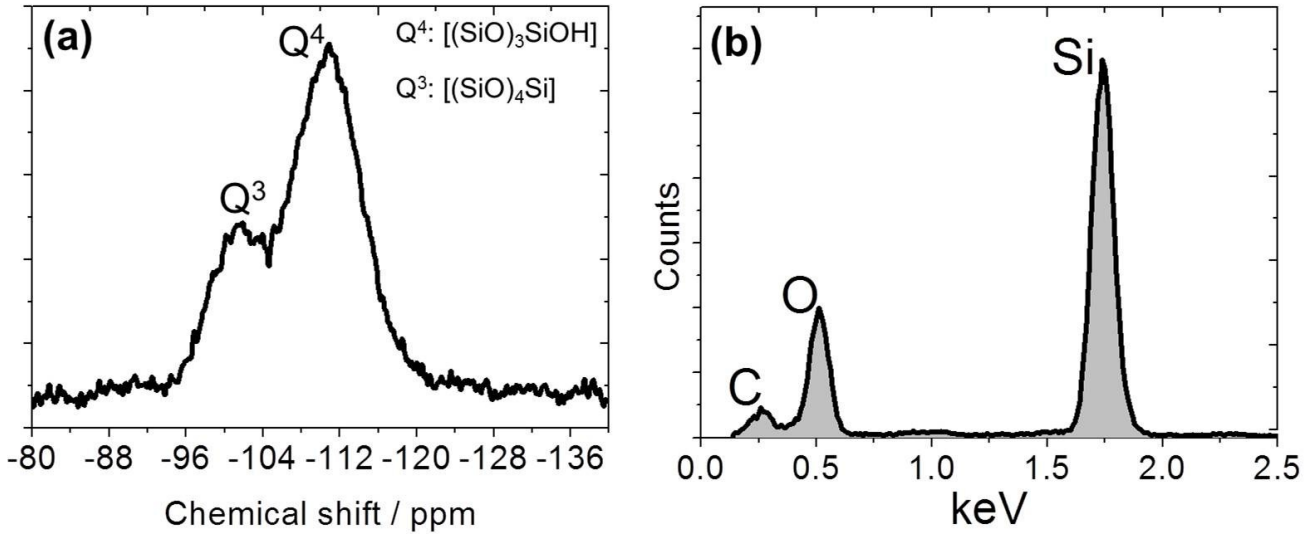

Fig. S 7 (a) Solid –state ^{29}Si NMR spectra and (b) elemental analysis using EDX of monodispersed NHSPs

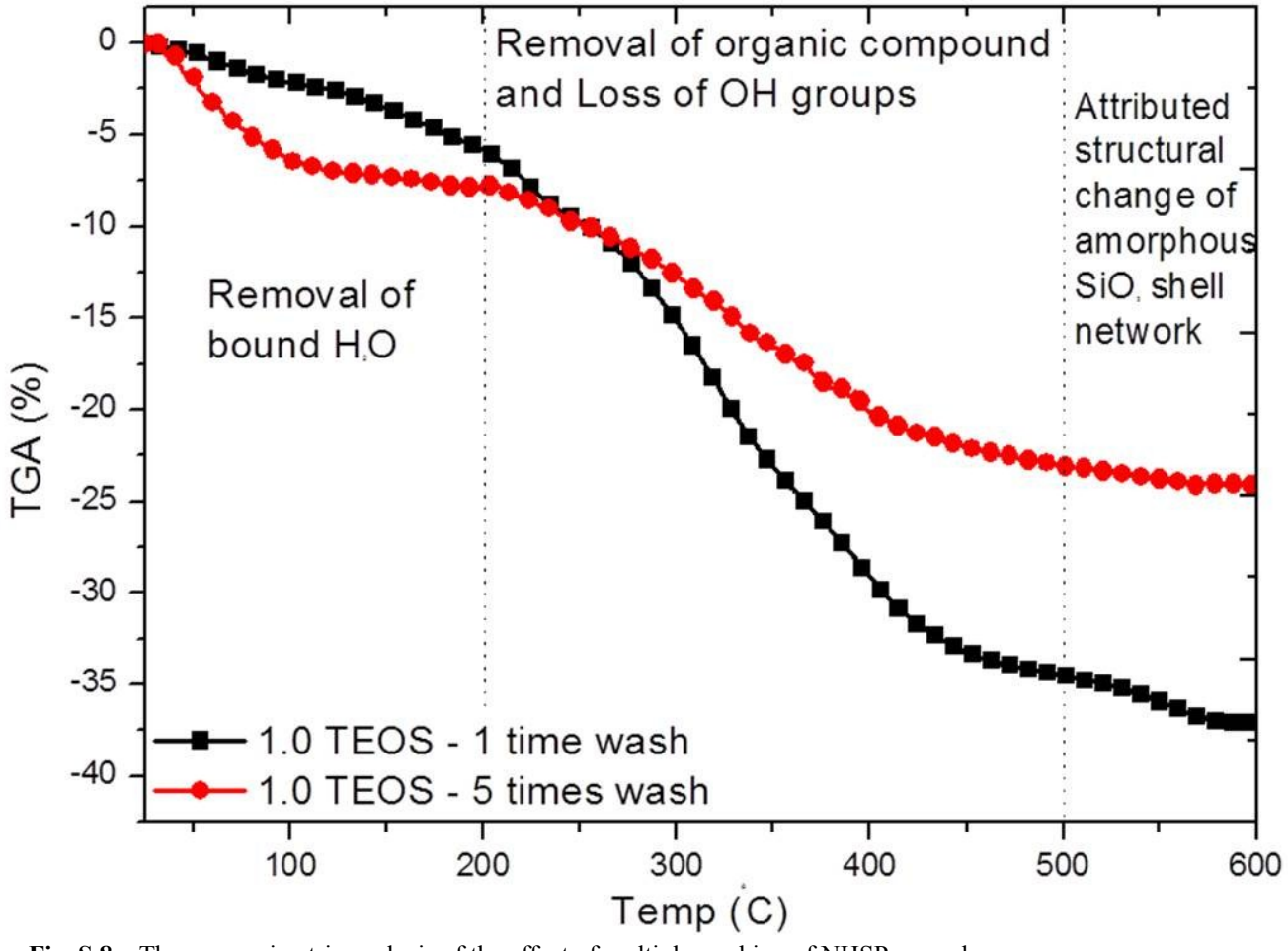

Fig. S 8 Thermogravimetric analysis of the effect of multiple washing of NHSPs samples

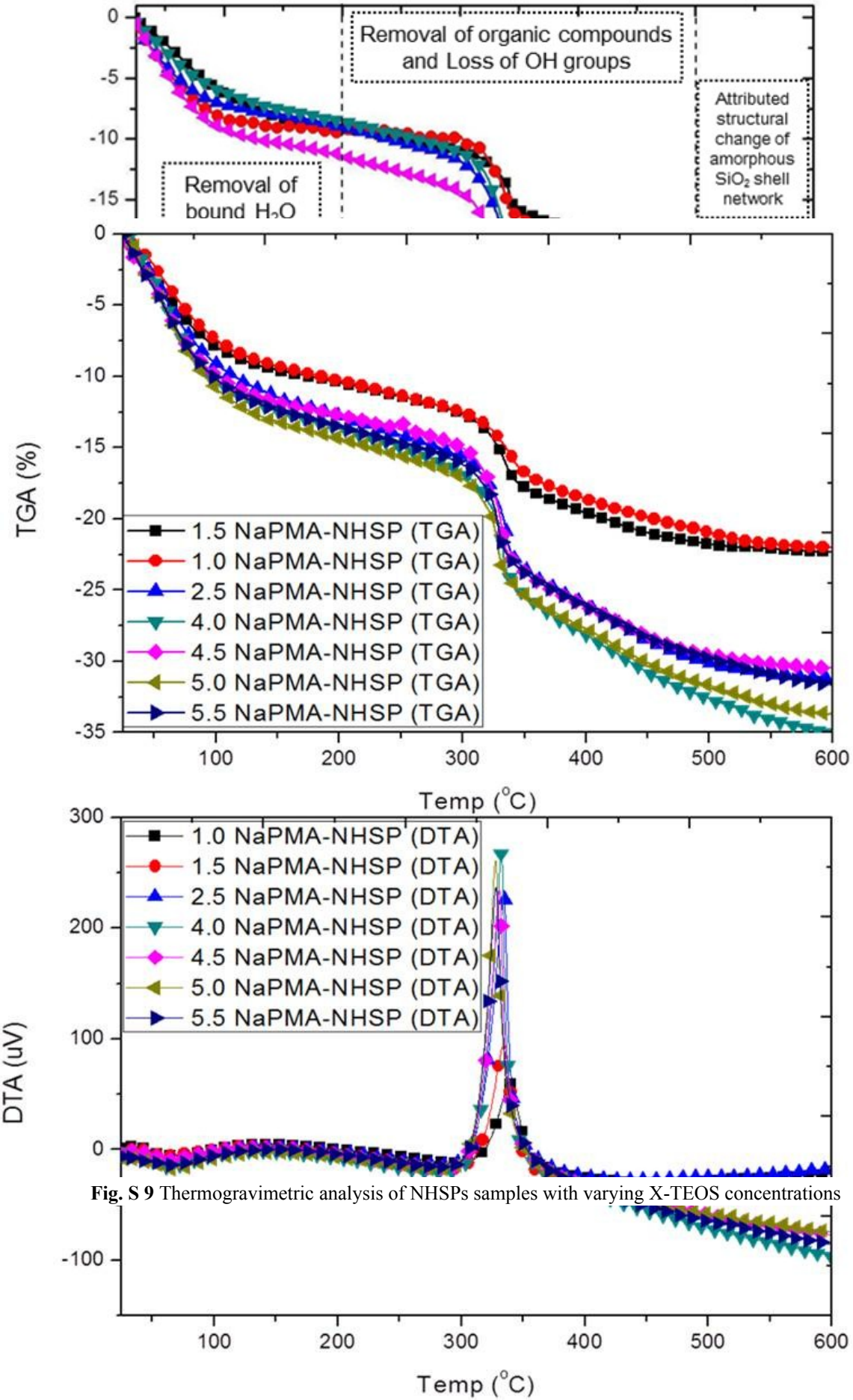

Fig. S 9 Thermogravimetric analysis of NHSPs samples with varying X-TEOS concentrations

Fig. S 10 Thermogravimetric analysis and differential thermal analysis of NHSPs samples with varying Y-NaPMA concentrations

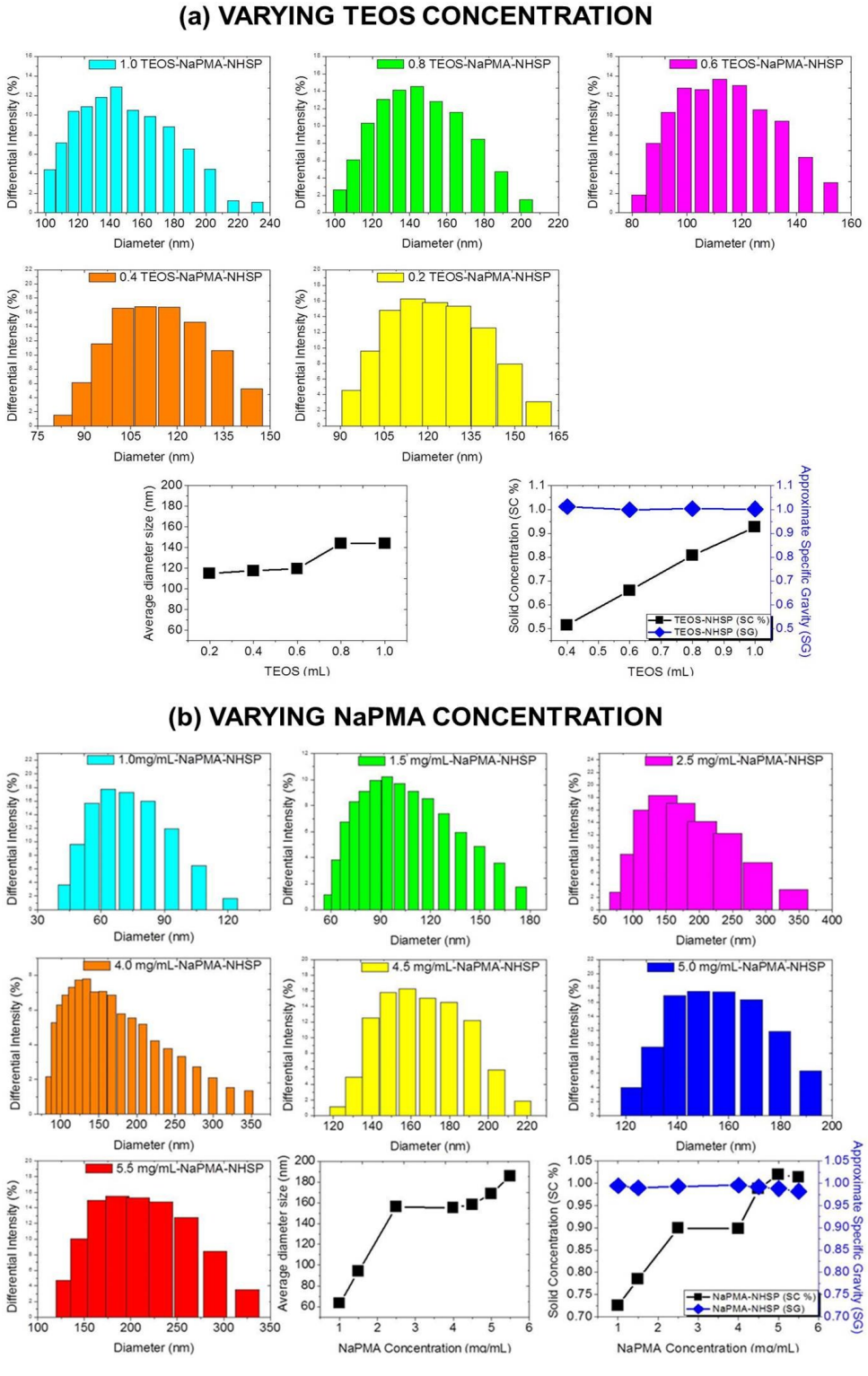

Fig. S 11 Particle size distribution of NHSPs powder samples with approximate specific gravity (sg) and average solid concentration with varying (a) X-TEOS and (b) Y-NaPMA concentrations.

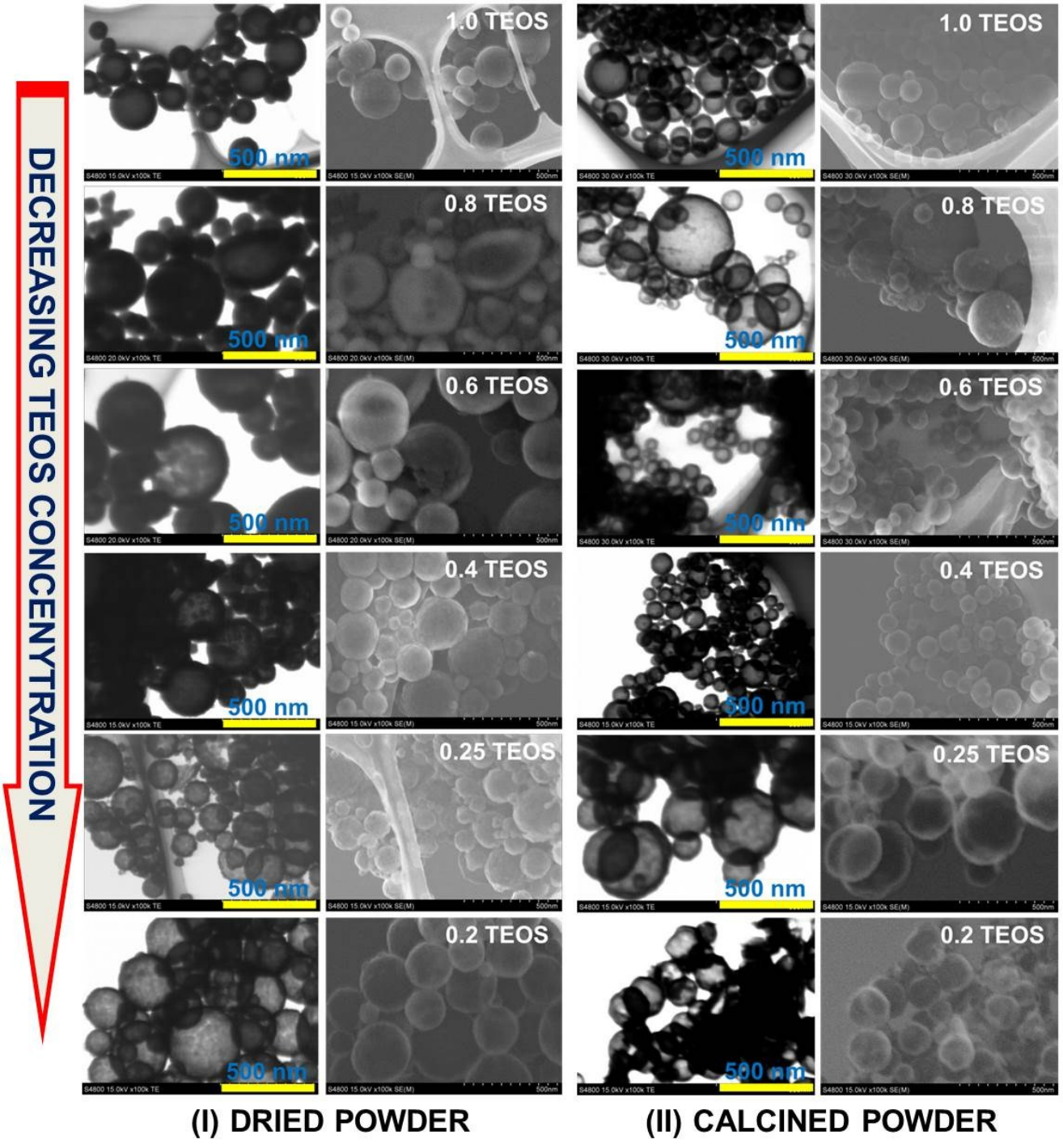

Fig. S 12 SEM images of (I) dried and (II) calcined-NHSPs samples with varying X-TEOS concentrations.

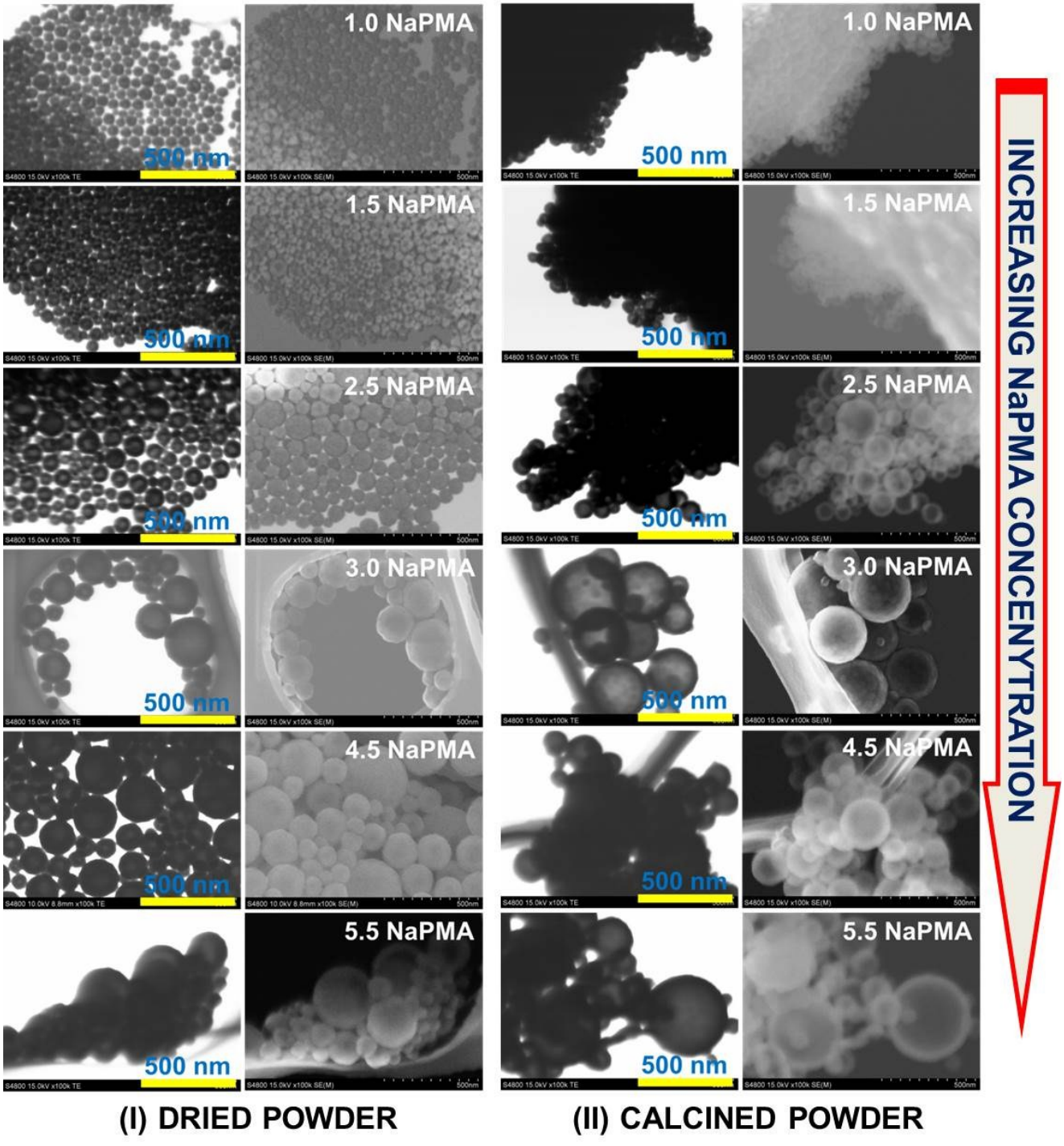

Fig. S 13 SEM images of (I) dried and (II) calcined NHSPs samples with varying Y-NaPMA concentrations

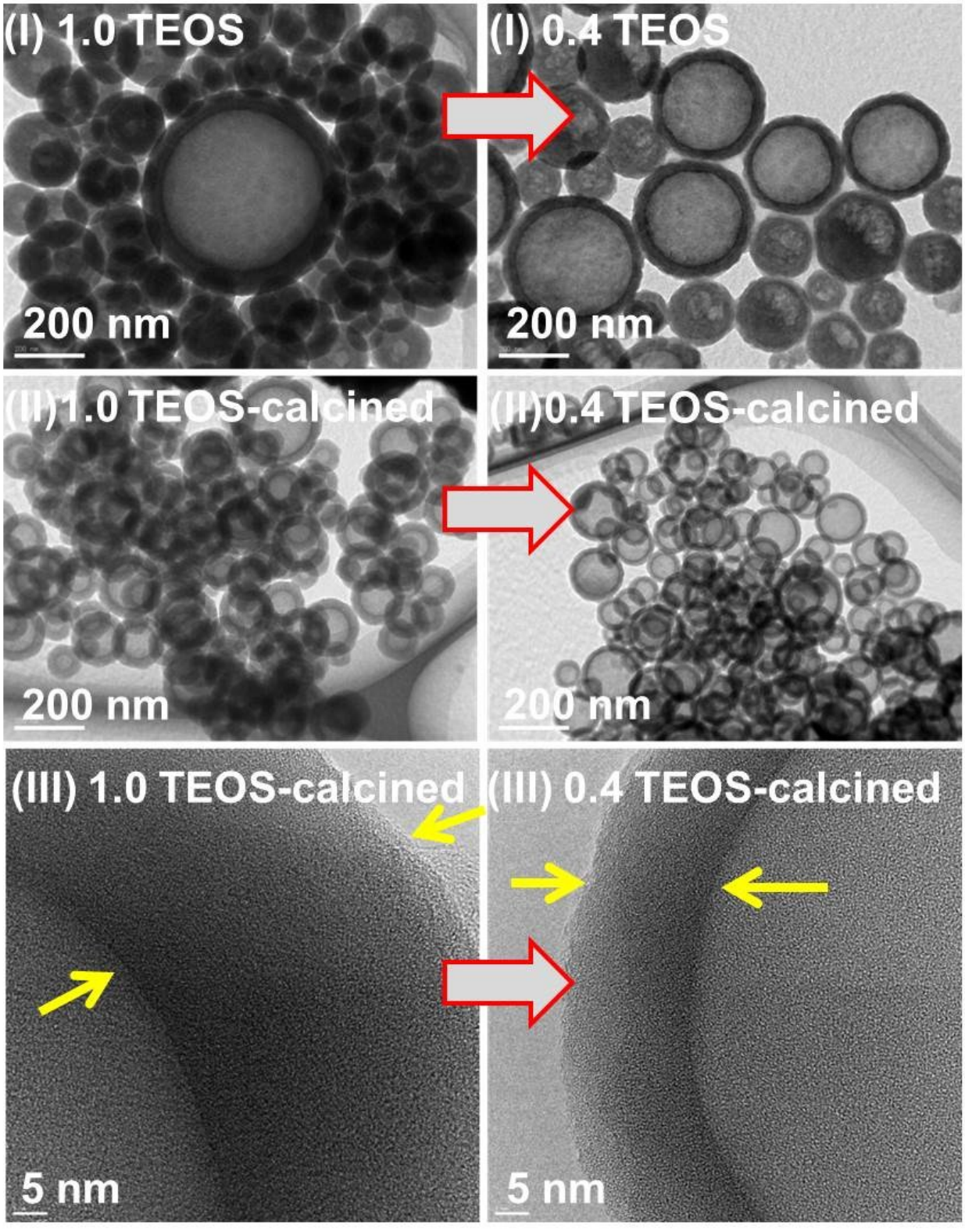

Fig. S 14 TEM images of (I) dried and (II, III) calcined NHSPs samples with varying X-TEOS concentrations.

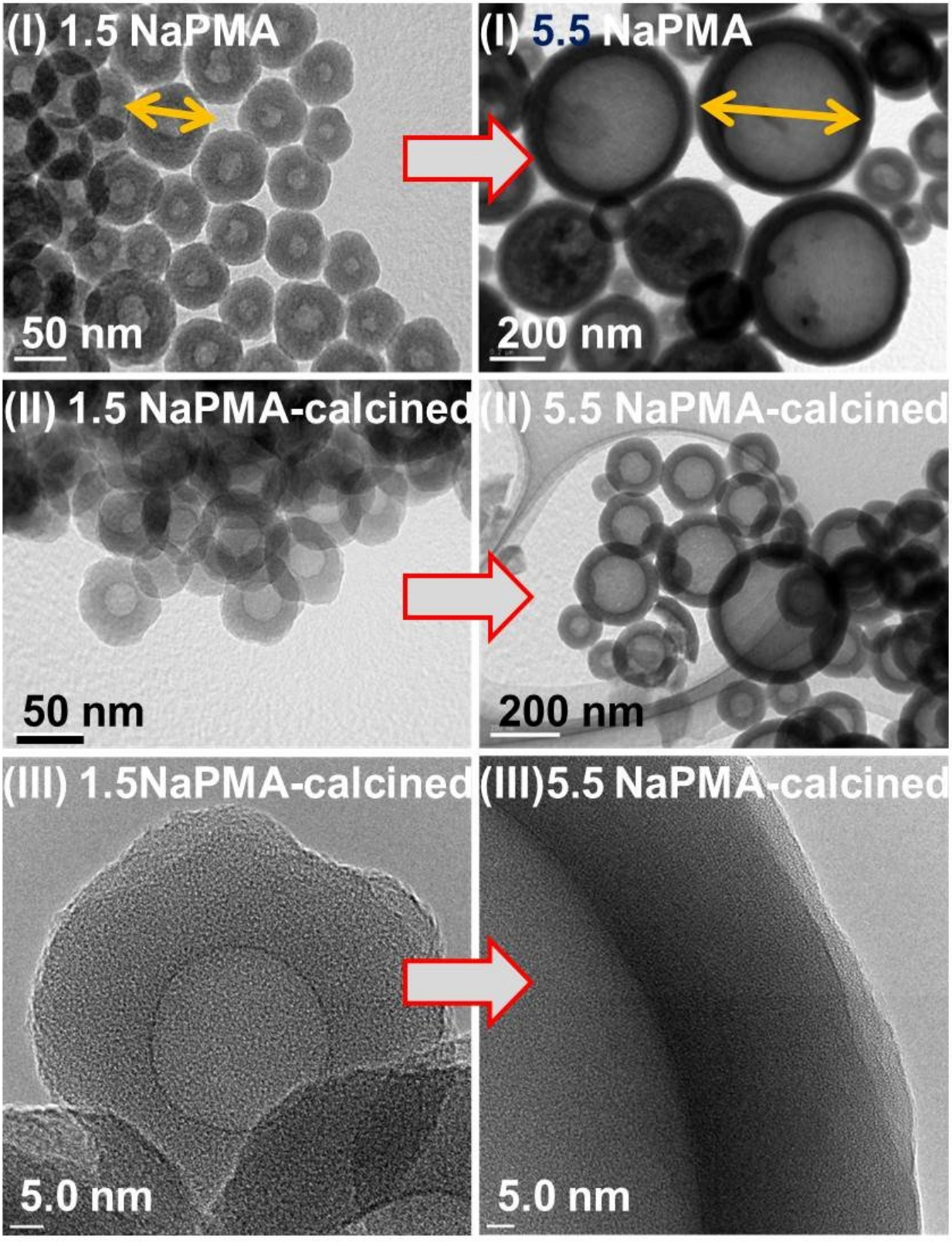

Fig. S 15 TEM images of (I) dried and (II, III) calcined NHSPs samples with varying Y-NaPMA concentrations

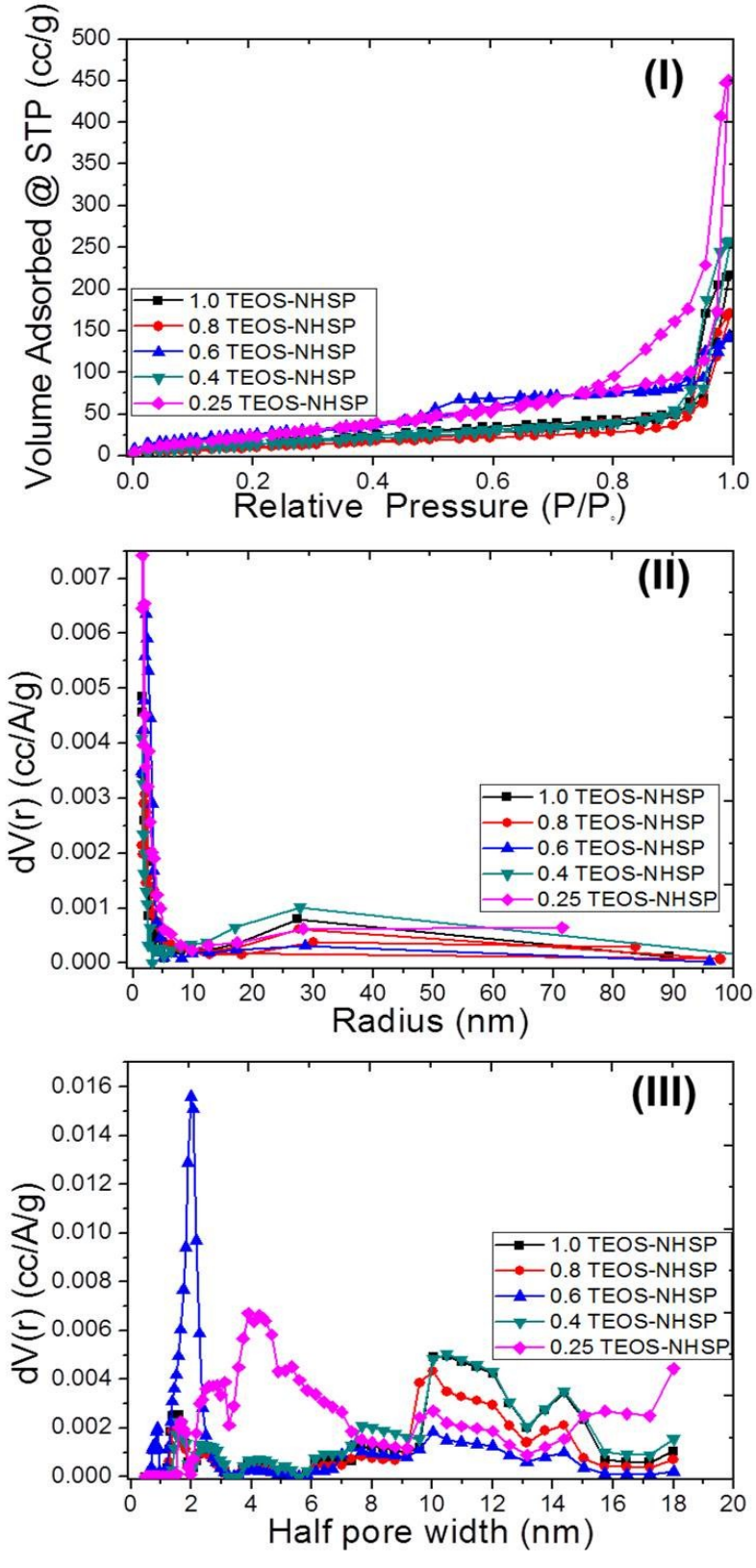

Fig. S 16 (I) N_2 adsorption-desorption isotherm with pore-size distribution calculated by (II) Barrett-Joyner-Halenda (BJH) method and (III) density functional theory (DFT) model of dried NHSPs samples with varying X-TEOS concentrations.

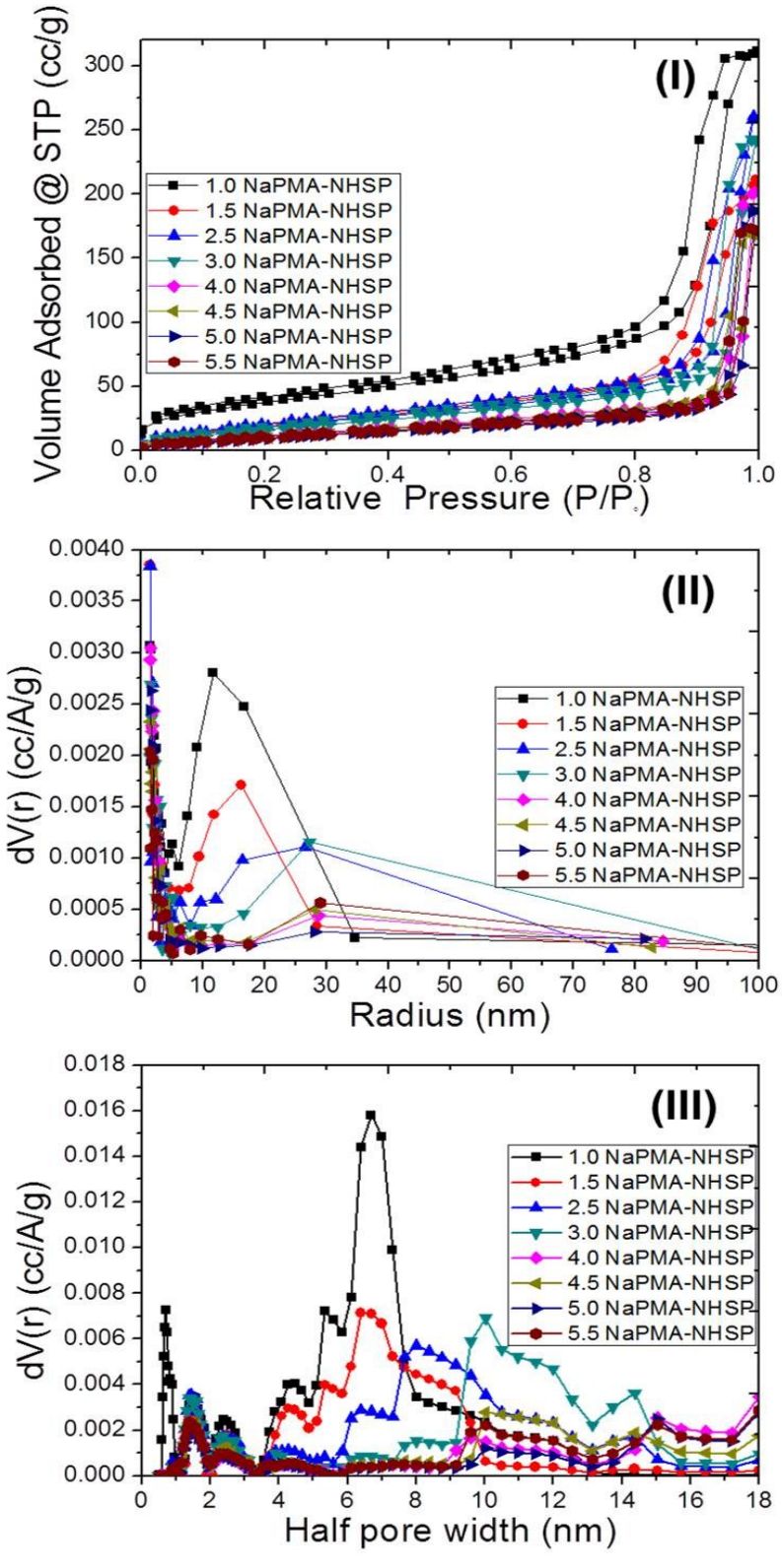

Fig. S 17 (I) N_2 adsorption-desorption isotherm with pore-size distribution calculated by (II) Barrett-Joyner-Halenda (BJH) method and (III) density functional theory (DFT) model of dried NHSPs samples with varying Y-NaPMA concentrations.

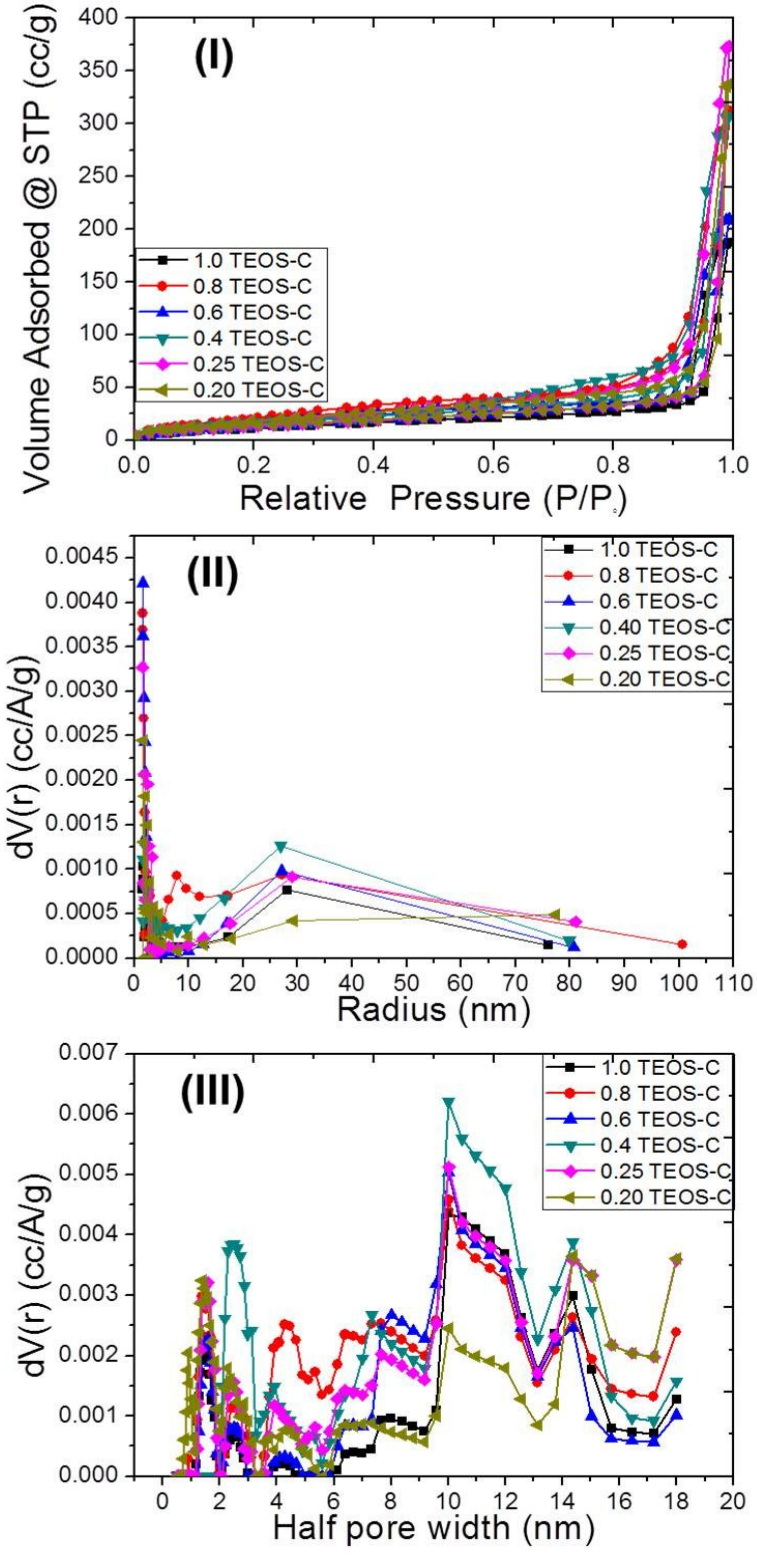

Fig. S 18 (I) N_2 adsorption-desorption isotherm with pore-size distribution calculated by (II) Barrett-Joyner-Halenda (BJH) method and (III) density functional theory (DFT) model of calcined NHSPs samples with varying calcined-X-TEOS-C concentrations.

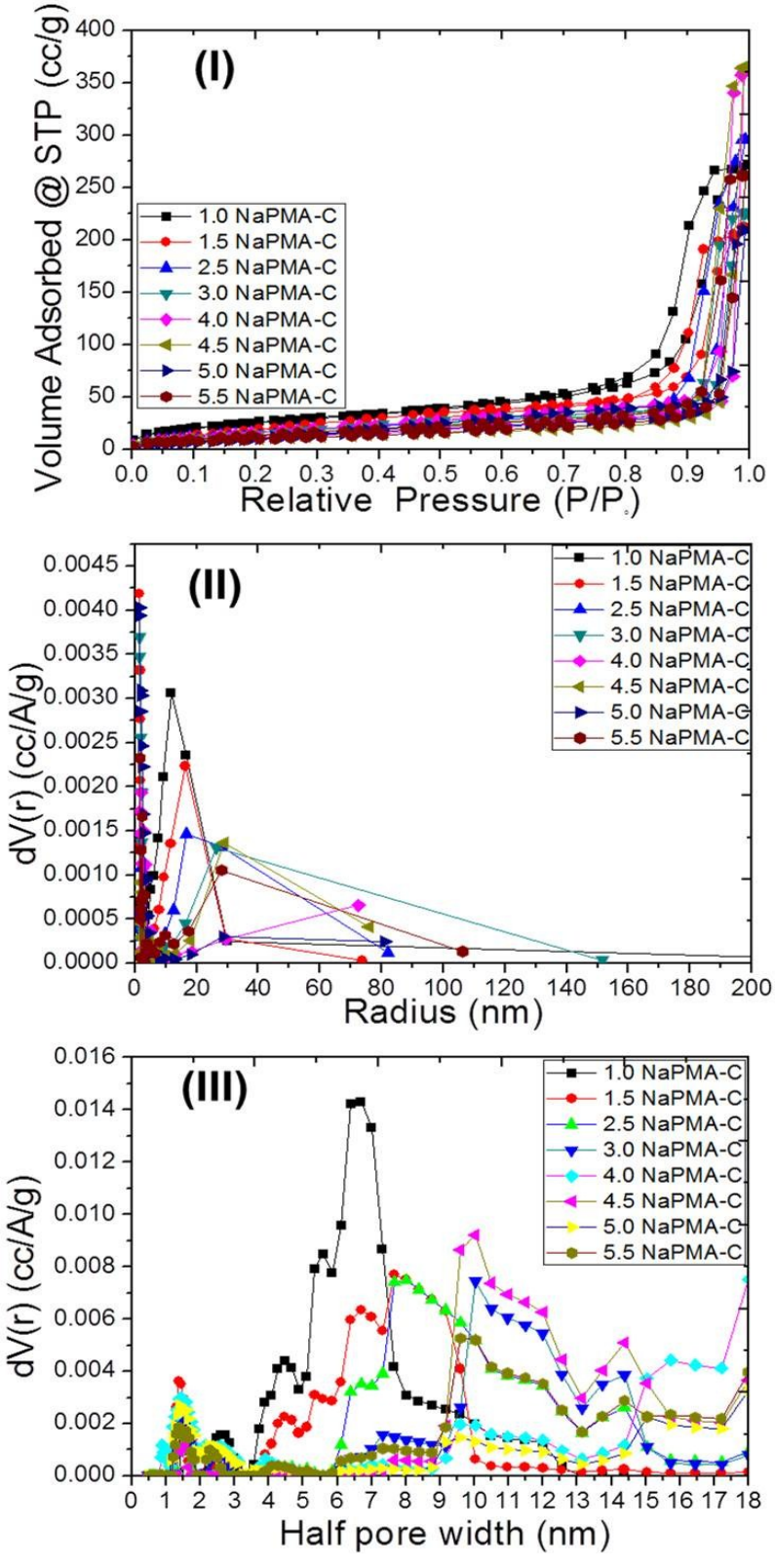

Fig. S 19 (I) N_2 adsorption-desorption isotherm with pore-size distribution calculated by (II) Barrett-Joyner-Halenda (BJH) method and (III) density functional theory (DFT) model of calcined-NHSPs samples with varying calcined -Y-NaPMA-C concentrations.

Table S 1 Physicochemical properties of dried NHSPs with varying X-TEOS concentrations.

NHSPs with TEOS concentration (non-calcined)	BJH Pore diameter (nm)	DFT Pore diameter (nm)	BET surface area (m^2g^{-1})	Pore volume ($cc\ g^{-1}$) $_{BJH}$	Pore volume ($cc\ g^{-1}$) $_{DFT}$
1.00	1.587	10.49	69.662	0.331	0.281
0.80	4.6	10.03	53.649	0.303	0.253
0.60	2.17	1.985	105.85	0.213	0.192
0.40	1.50	10.49	79.702	0.416	0.330
0.25	1.59	3.898	109.33	0.694	0.440
0.20	1.9	3.7	89.119	0.788	0.749

Table S 2 Physicochemical properties of calcined-NHSPs with varying calcined X-TEOS-C concentrations.

NHSPs with TEOS concentration (calcined)	BJH Pore diameter (nm)	DFT Pore diameter (nm)	BET surface area (m^2g^{-1})	Pore volume ($cc\ g^{-1}$) $_{BJH}$	Pore volume ($cc\ g^{-1}$) $_{DFT}$
1.00	1.591	10.03	54.14	0.277	0.236
0.80	1.588	10.03	96.01	0.464	0.354
0.60	1.58	10.03	68.7	0.314	0.266
0.40	1.73	10.03	66.98	0.465	0.390
0.25	1.50	10.03	52.69	0.572	0.363
0.20	1.589	14.37	55.086	0.513	0.264

Table S 3 Physicochemical properties of dried NHSPs with varying Y-NaPMA concentrations.

NHSPs with NaPMA concentration (non-calcined)	BJH Pore diameter (nm)	DFT Pore diameter (nm)	BET surface area (m^2g^{-1})	Pore volume ($cc\ g^{-1}$) $_{BJH}$	Pore volume ($cc\ g^{-1}$) $_{DFT}$
1.0	1.5	6.69	138.6	0.459	0.467
1.5	1.5	6.39	77.72	0.322	0.291
2.5	1.5	8.00	76.82	0.395	0.330
3.0	1.589	10.03	66.852	0.366	0.339
4.0	1.589	17.99	47.012	0.310	0.186
4.5	1.588	10.03	43.124	0.288	0.196
5.0	1.588	17.99	41.713	0.288	0.158
5.5	1.503	17.99	42.11	0.261	0.195

Table S 4 Physicochemical properties of calcined-NHSPs with varying calcined Y- NaPMA-C concentrations.

NHSPs with NaPMA concentration (calcined)	BJH Pore diameter (nm)	DFT Pore diameter (nm)	BET surface area (m^2g^{-1})	Pore volume ($cc\ g^{-1}$) $_{BJH}$	Pore volume ($cc\ g^{-1}$) $_{DFT}$
1.0	11.74	6.69	98.325	0.409	0.408
1.5	1.5	7.65	85.345	0.319	0.308
2.5	16.597	8.01	48.79	0.452	0.383
3.0	1.50	10.03	65.12	0.341	0.319
4.0	1.89	17.99	44.503	0.553	0.293
4.5	28.95	10.03	38.772	0.563	0.429
5.0	1.502	17.99	58.252	0.324	0.172
5.5	1.504	9.587	37.685	0.404	0.321

.**Table S 5** Thermal conductivity values of different types of glass

Different types of glass	Thermal conductivity (W/m K) based from the references*
Lead (glass)	**1.2**
Pyrex (borosilicate)	**1.3**
Soda lime (glass) (20 ^{o}C)	**1.1**
Soda lime (glass) (93 ^{o}C)	**1.3**

*[1] Incropera F P 2007 *Fundamentals of heat and mass transfer* (Hoboken, NJ: Wiley)

*[2] Matthews L, Viskanta R and Incropera F 1984 Development of inverse methods for determining thermophysical and radiative properties of high-temperature fibrous materials *International Journal of Heat and Mass Transfer* **27** 487-95

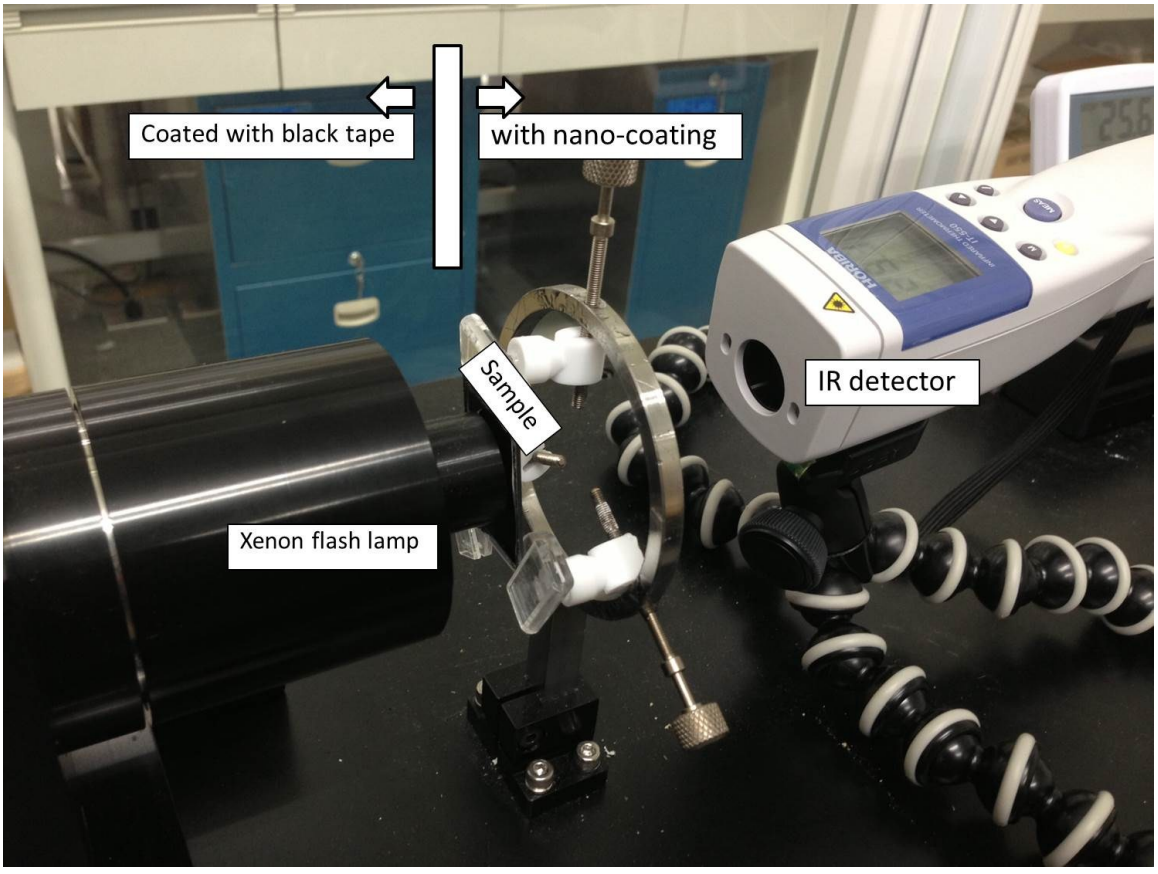

Fig. S 20 A typical xenon flash lamp thermal characterization set up.

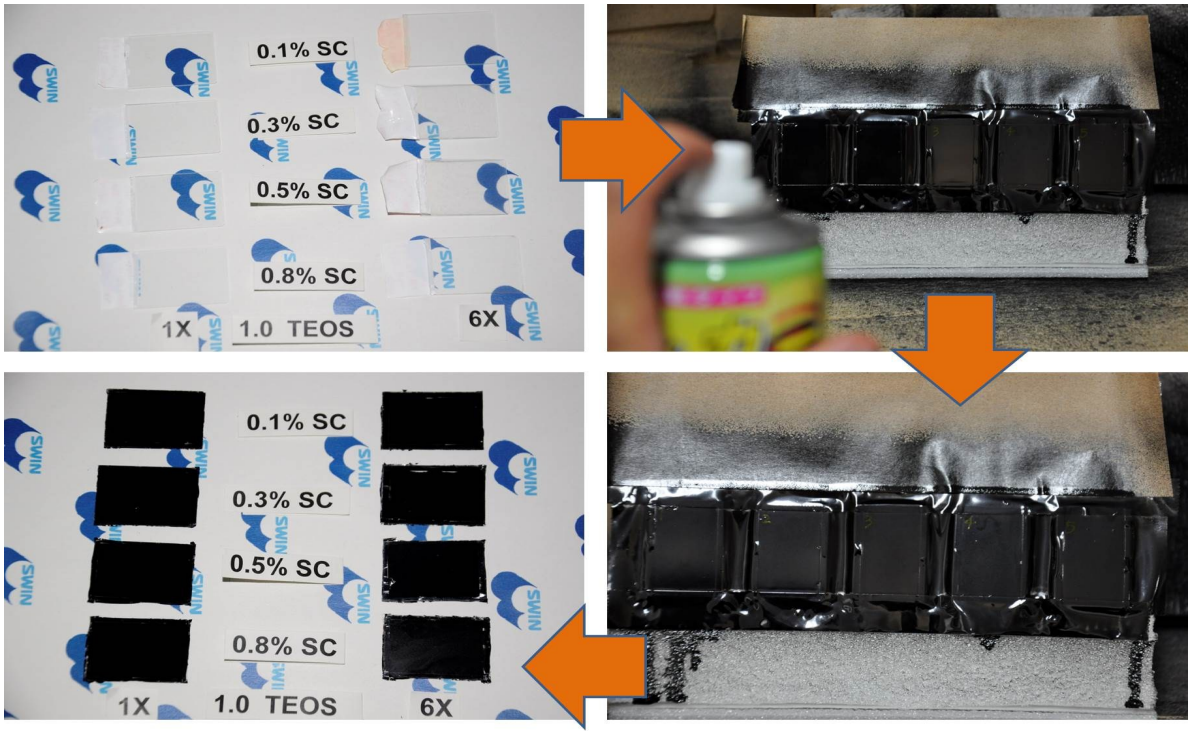

Fig. S 21 Test samples sprayed with carbon paint for thermal characterization using the xenon flash lamp set-up

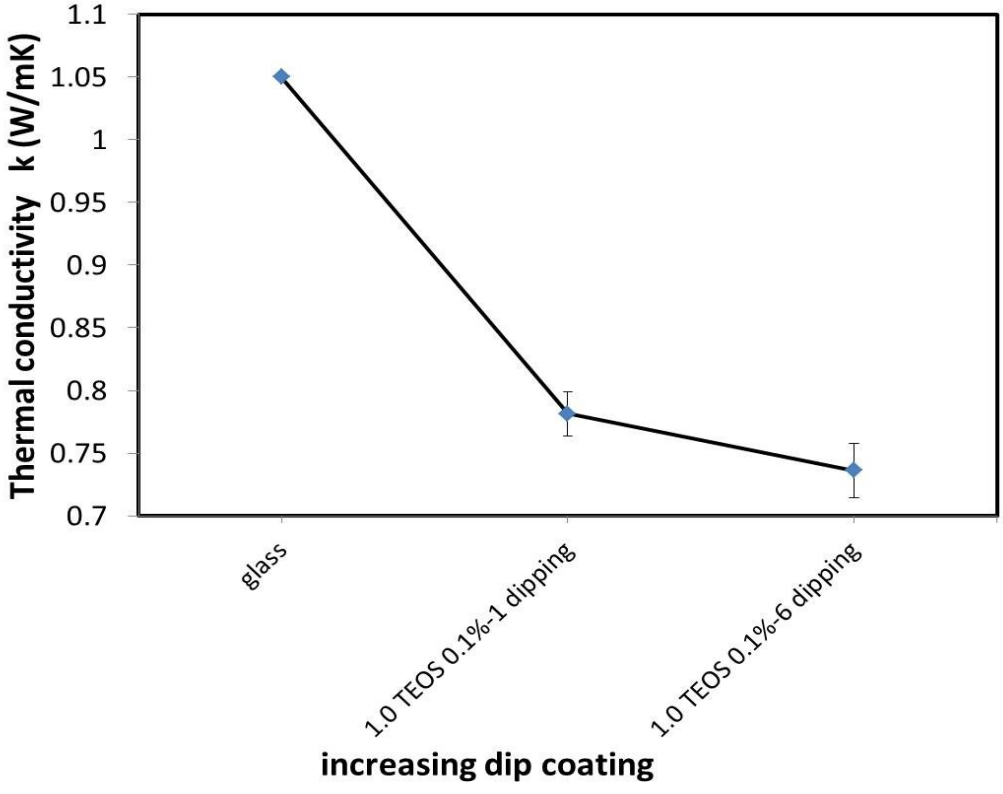

Fig. S 22 Thermal conductivity values of 0.1 % solid concentration NHSPs coated glass samples with increasing number of dippings

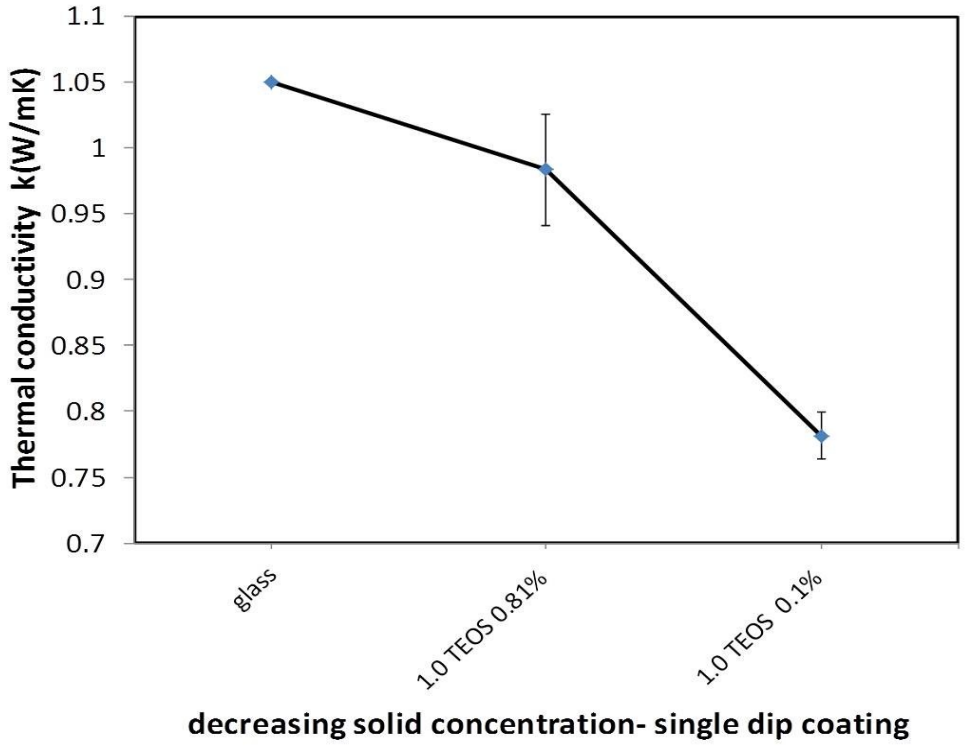

Fig. S 23 Thermal conductivity values of NHSPs coated glass samples with decreasing solid concentration of NHSPs in dip coating solutions

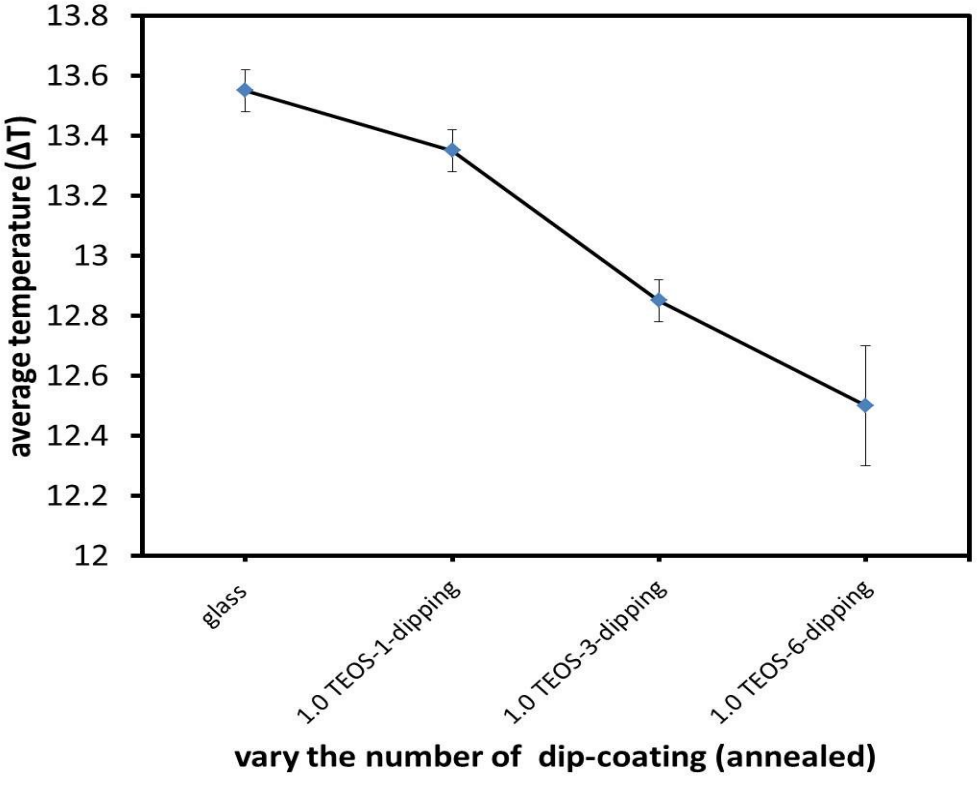

Fig. S 24 Average surface temperature change before and after xenon lamp flashing with respect to the number of dippings in 0.10% solid concentration

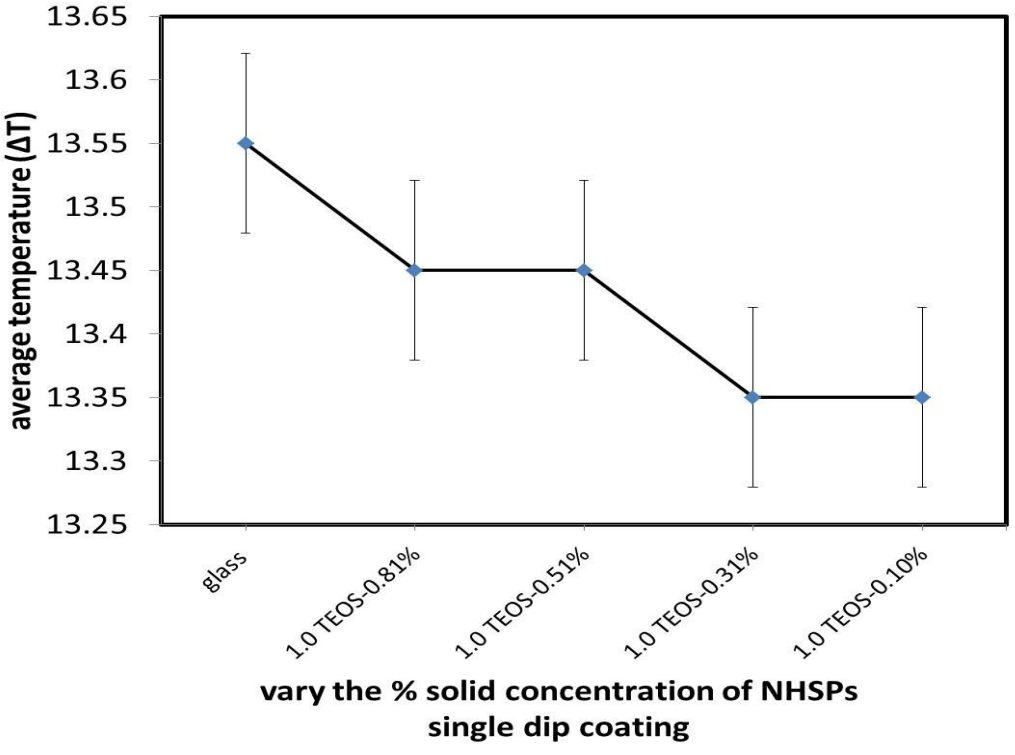

Fig. S 25 Average surface temperature change before and after xenon lamp flashing with decreasing NHSPs in dip coating solutions

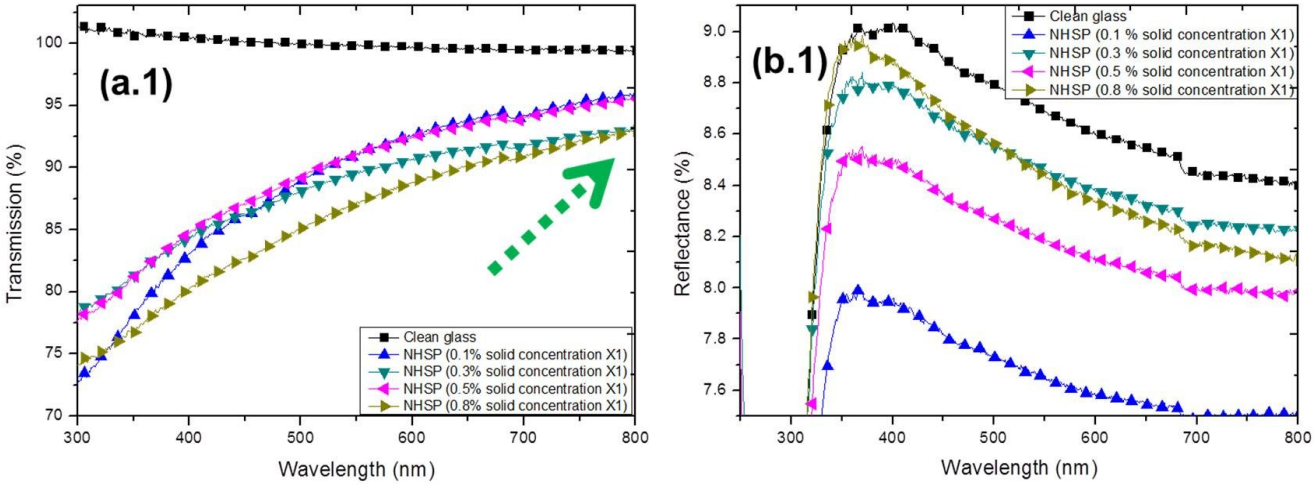

Fig. S26 Transmittance (a.1) and Reflectance (b.1) of the glass substrate coated by NHSP (0.1% solid concentration) prepared by dip coating at (single immersion only) at different solid concentration.

Table 6S.

Sample material	Thermal conductivity (W $m^{-1}K^{-1}$)	Standard deviation	% difference compared to glass
Glass substrate	1.05		
1.0 TEOS-0.1%-1x	0.78	0.0176	25.6
1.0 TEOS-0.1%-6x	0.74	0.0217	29.9

Table 7S

Sample material	Thermal conductivity (W $m^{-1}K^{-1}$)	Standard deviation	% difference compared to glass
Glass substrate	1.05		
1.0 TEOS-0.1%-1x	0.98	0.0420	6.50
1.0 TEOS-0.1%-6x	0.78	0.0176	25.6